International Journal of Coal Science & Technology (2024) 11:18
https://doi.org/10.1007/s40789-024-00668-y

RESEARCH

Performance characteristics of the airlift pump under vertical solid–water–gas flow conditions for conveying centimetric-sized coal particles

Parviz Enany[1] · **Carsten Drebenshtedt**[1]

Received: 2 December 2022 / Revised: 18 August 2023 / Accepted: 2 February 2024

Abstract
In this study, the installation of an airlift pump with inner diameter of 102 mm and length of 5.64 m was utilized to consider the conveying process of non-spherical coal particles with density of 1340 kg/m^3 and graining 25–44.5 mm. The test results revealed that the magnitude of increase in the solid transport rate due to the changes in the three tested parameters between compressed air velocity, submergence ratio, and feeding coal possibility was not the same, which are stand in range of 20%, 75%, and 40%, respectively. Hence, creating the optimal airlift pump performance is highly dependent on submergence ratio. More importantly, we measured the solid volume fraction using the method of one-way valves in order to minimize the disadvantages of conventional devices, such as fast speed camera and conductivity ring sensor. The results confirmed that the volume fraction of the solid phase in the transfer process was always less than 12%. To validate present experimental data, the existing empirical correlations together with the theoretical equations related to the multiphase flow was used. The overall agreement between the theory and experimental solid delivery results was particularly good instead of the first stage of conveying process. This drawback can be corrected by omitting the role of friction and shear stress at low air income velocity. It was also found that the model developed by Kalenik failed to predict the performance of our airlift operation in terms of the mass flow rate of the coal particles.

Keywords Vertical velocity · Non-spherical particle · Submergence ratio · Three-phase flow · Churn flow · Superficial velocity

1 Introduction

An airlift pump, a simple device for thrusting liquids and sometimes liquid–solid mixture vertically, demands compressed air injection. The mechanism is typically based on making changes initially in the density of a liquid–solid mixture inside a riser pipe by injecting compressed air (Kalenik and Chalecki 2018). Then, the drag force created between the small air bubbles and the water-particle phases helps the three-phase mixture to move upward. Due to its very simple structure, low primary cost, and no need for continuous maintenance, this pump is widely utilized in various industrial systems, such as the processes in municipal wastewater treatment, the neutralization of acidic mine water drainage, the transfer of nuclear reactor effluents, and the extraction of ocean floor sediments. The single disadvantage of airlift pumps, compared to other conventional ones in this area, is their low efficiency, which typically becomes much more evident in the cases where they are not sufficiently submerged in water.

Various ideas have been so far raised to improve the efficiency of this pump, and optimize this device for two-phase (air–water) flows, but unfortunately nearly all have not been evaluated in three-phase (air–water-solid) flows. In this respect, Kumar et al. (2003) employed a tapered pipe with an expanding diameter from bottom to top, and found that the pump efficiency had enhanced because the air bubbles had agglomerated later. This idea was afterward tested with a novel design of the pump by Zaraki et al. (2016) on two-phase flows. In airlifts using the radial air injection method (air jacket), Enany et al. (2021)

✉ Parviz Enany
parviz.enany@doktorand.tu-freiberg.de

[1] Faculty of Mining and Special Civil Engineering, Technische Universität Bergakademie, Gustav-Zeuner Straße 1A, 09599 Freiberg, Germany

further revealed that compressed air injection in parallel with the air jacket could boost the pump efficiency in water transfer. This idea was also further evaluated by Kassab et al. (2022) for water transfer purposes.

The presence of different regimes in vertical motions has also led to the possibility of recruiting theoretical correlations, consistent with this pump, under certain conditions. Accordingly, Yoshinaga and Sato (1996) provided a new formula to estimate the airlift pump performance based on the conservation of momentum for slug flow regimes. To this end, a small pump with a fixed inlet particle flow rate was used in order to confirm its equation. On the other hand, understanding the transfer rates of solid particles and inlet air rates was raised as one of the main prerequisites for using the suggested model, which involved the construction of a pump and its evaluation following some experimental tests.

Given the fact that liquids are the main transporter phase of solid particles, Margaris and Papanikas (1997) presented a correlation in which the interaction of the forces between air bubbles and solid particles, as well as the particular shape of the bubbles was neglected. Generally, their outcomes were suitable in determining the optimal values for the pipe diameter and length, as well as the injection air level. It should be noted that, Enany et al. (2022) in their research on three different particles, in spherical, semi-spherical, and irregular shapes, demonstrated that water and air contributed to upward transfer of the solid particles in the churn flow regime. Therefore, the equation offered by Margaris & Papanikas needs to be modified for the churn flow regime conditions.

As mentioned above, airlifts are often used to transfer fine solids up to a few millimeters (sediments deposited on lakes, sea, and ocean beads). Even most practical research has been conducted not only on small size but also in spherical shape format (e.g., Kato et al. 1975; Fujimoto et al. 2010; Sadatomi et al. 2013; Kalenik and Chalecki 2018; and Wang et al. 2020). Since round particles are very rare in the industry and real projects, paying more attention to higher-dimensional particles without a geometric shape can lead to increased use of this pump in transferring of solid particles, such as mining ores.

Since it is almost impossible to install any kind of sensor inside the riser pipe to measure the characteristics of multiphase flows, especially when there is a solid phase, in the last two decades, the utilize of fast speed cameras to analyze such flows has become more prevalent in scientific articles (e.g., Fujimoto et al. 2010; Abed et al. 2018; Wang et al. 2020; and Kassab et al. 2022). To analyze the flow regime, at least two cameras should be installed because the bubbles agglomeration along the vertical tube does not always remain constant. This case is often not considered due to the difficulty of interpreting the results.

With respect to the previously cited works, it should be noted that most researchers have paid less attention to the effects of two cases when conducting experiments to measure the amount of pump power in the solid particle transfer. The first case is to regulate the rate of solid particle inflow, which is in total contrast to the actual conditions of the pump in the solid particle suction process. For the sake of example, please see the research conducted by Kato et al. (1975), Weber (1974), Margaris and Papanikas (1997), Mahrous (2012), and Hu et al. (2012). The second case is less attention to the decreased submergence ratio during the sampling of solid particles, which leads to a gradual decrease in the pump efficiency in carrying solid particles. The effects of this case become much more evident on the laboratory scale (Ramdhani et al. 2020; Yulistiansah et al. 2020), especially in cases where the water reservoir size is small. Therefore, the offered design by Kassab et al. (2007) and Fujimoto et al. (2003) studies are recommended to overcome this weakness.

This study aimed to obtain the optimal rate of solid particle outflow to ensure the operability of the airlift pump for centimetric-sized particles. To this end, we used non-spherical coal particles, grinding 25–44.5 mm. In addition, the inlet air flow velocity, submergence ratio (the ratio between the submerged length of the riser e and its total length), and feeding solid possibility (maximum solid weight considered for testing) were also considered as the variable parameters. Also, to compare practical results with theoretical equations, the volume fraction of coal was measured with one-way valves (backflow prevention).

2 Materials and method

The schematic of the airlift pump to be studied experimentally and theoretically here is displayed in Fig. 1. The pump body consisted of six main parts, which included a sump, a suction pipe of length (h_S), an air injector, a riser pipe of length (h_R), a separator tank and a water reservoir (downcomer) from the bottom. The riser pipe was made up of transparent hard plastic with an inner diameter of 102 mm in order to allow for the visual observation of the particle transfer. The 4.37-m-long pipe contained two similar pieces connected to each other with a flange. The inlet was further connected to the air injector from one side, and its outlet was connected to the metal separator tank. The suction pipe was about 1.27 m with an inner diameter of 102 mm, and its entrance was about 20 mm from the sump bottom. Compressed air was being injected radially into the riser pipe by means of a perforated pipe around which 80 holes with a diameter of 3 mm were regularly drilled. Unlike conventional methods, compressed air was blown parallel to the air jacket outer wall, and did not hit it directly. As proven in the previous research by the authors, that given method

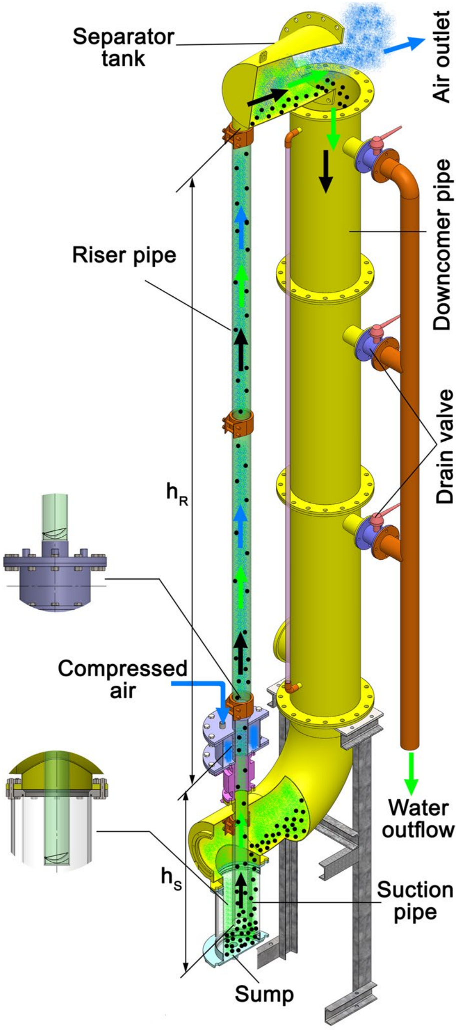

Fig. 1 Schematic of the working principle of the airlift pump

showed a better performance due to the entry of air and the equal use of all the holes in the jacket. The Additional file 1: Fig. S1 depicts the schematic structure of the air injector. In the top of the pump, i.e., in the separator tank, the injected air was also separated from the water-particle mixture, released into the environment, and then water and solid particles were poured into the water reservoir. The solid particles subsequently fell into the downcomer only by gravity, and returned to the sump (entrance suction pipe). Of note, two drain valves connected to the water reservoir body are always used to adjust the value of the submergence ratio ($S_r = h_w/h_R$). As observed in Fig. 1, the pump is designed in such a way that water and solids flow in a closed cycle, so there are no changes in the submergence ratio and solid weight during the tests and water is permanently reusable.

The non-spherical particle applied in the study was coal with the absolute density of 1340 kg/m^3, the loose bulk density of 726.5 kg/m^3, and the graining of 25–44.5 mm. Beyond the examination time, the tested particles were soaked in a separate container, so that there was no weight difference between the dry and saturated particles all through the test process.

Initially, a fixed amount of coal (25, 30, 35 kg) was placed in the pump, and the desired submergence ratio (S_r) was provided by adding water. Then, a three-phase upward flow began by injecting compressed air and lowering the specific gravity of the mixture before and after the air jacket. As mentioned in the research objectives, one of the important parameters in this study was to evaluate the role of compressed air to pump coal particles. To this end, the compressed air was gradually compounded in order to reach a state where the maximum level of solid particles could be pumped per unit time by keeping the submergence ratio fixed. Considering the compressor output power, it was also possible to inject more than 250 m^3/h of compressed air, but the coal particles could hit the separator tank wall at a very high speed, and were often destroyed with excessive injection of compressed air. Thus, the maximum velocity of compressed air injection was considered equal to 2.72 m/s at $S_r = 0.6$ to avoid the occurrence of such conditions and above all keep the dimension of the particles uniform. An electric sensor made by the IFM Co. was further utilized to record the amount of compressed air injected with an accuracy of 2%, which was then installed between the on/off valve and the air injector.

An Optiflux induction sensor with an accuracy of 0.5% was used to measure the water velocity before the air injection level. The feeding coal possibility was directly correlated with their mass flow rate in the pumping process. The increase in the amount of coal inside the pump continued until it did not cause excessive accumulation of particles in the sump, as an increase in the weight of the particles piling up on each other would reduce the suction force of the pump and prevent more particles to entering the suction pipe.

In our previous study, we showed that the best efficiency of the pump in a two-phase flow (air–water) is achieved in the submergence range between 0.6 and 0.75. However, for a centimeter-sized particle, this level should be raised to 0.8 for faster transfer and onset of movement with less compressed air consumption (Enany et al. 2023, 2022). Therefore, to understand the effects of S_r on the pump efficiency in three-phase conditions, three submergence ratios of 0.6, 0.7, and 0.8 were considered. Of note, due to the increase in submergence level after injecting compressed air (Al-Maliki 2014), the capacity of the water tank for solid sampling was not sufficient if the S_r raised to 0.9.

For sampling, the transferred solid particles were collected by placing a flexible mesh with 1 mm cubic holes at the outlet of the separator tank. This did not prevent the water from passing through and purring to the downcomer. According to the results of frequency analysis (see

Additional file 2: Fig. S2), the duration of the sampling was set to 15 s, which is long enough to measure the time-averaged values. The collected particle weights were measured after 4 min to minimize the effects of the water droplets that remained on the particles. According to the information in Fig. 1, the amount of water in the downcomer is always four times the amount in the flow, and the sampling time does not adversely affect the change in the submergence ratio. After each sampling and weight measurement, the particles were poured into the downcomer so that there was no change in the value of solid particles inside the pump for the following sampling.

In this section, we describe how to measure the amount of particle volumetric fraction in the suction and riser pipe. Since we face two different types of multiphase flow in time of solid particle transportation by an airlift pump, it is a bit tricky to measure the particle volumetric fraction directly, and the process is not an error-free task. In a studies that conducted with Minagawa et al. (2007) and Wang et al. (2020), they used the fast-imaging technique to analyze the particle volumetric fraction, in which the number of the particles recorded in video images was counted. Due to the inconstant bubble agglomeration as they move upward, a permanent change in the share of each phase is inevitable. On the other hand, the overlap of solid particles during two-dimensional imaging also indicates that, unfortunately, the fast-imaging technique in estimating the actual volume of particles for transfer is not able to extend the results to the entire length of the pump. To estimate the optimal volume fraction of the solid phase to be transferred by the pump, we used a new and simpler method that, according to the author, has not been seen in any other research.

To measure the coal volumetric fraction in the two main parts of the pump, a total of two one-way valves (backflow prevention) were employed at the inlet of the suction and riser pipe, where their position is shown in Fig. 1. The valves had no springs and no additional pressure was required to open them toward the main flow. According to the results of the water pumping examination, the two valves had no negative impact on the water velocity on average. It should be mentioned that the conditions of the three main variable parameters at the time of conducting this test were entirely similar to those arranged for the coal transportation sampling tests.

After the coal particle transportation stabilized, as the compressed air flow stopped immediately, one-way valves closed the entrance and suspended coal particles fell along the path to the suction and riser pipe entrance due to gravity and piled up on each other. Then, to define the bulk volume, the height of the accumulation of coal particles was measured accurately.

As the mean bulk volume of the particles was known a priori, the volume fraction was easily calculated. Additional file 3: Video S1 shows the mechanism of the one-way valve in this investigation. The interesting point is that the solid particles were moving in the center of the tube and did not collide with the one-way valve, which can be clearly seen in this video.

It is worth nothing that due to the inclination of the separator tank, it was not possible for coal particles to return to the riser pipe, so the measured height is associated with the particles that were present along the vertical path (from the inlet of the suction pipe to the upper part of the riser pipe). In total, fifteen measurements were carried out in each test series and the arithmetic mean values were used as a final result.

3 Results and discussion

The main objective of the practical tests here was to evaluate the optimal airlift pump performance for conveying cm-sized particles. For this purpose, three variable parameters were considered: air injection velocity, submergence ratio (S_r) and feeding solid possibility (F_s). As discussed in detail above, the mass flow rate of the coal particles (M_s) was measured by the discharged coal mass and 15 s sampling time, whose measurement uncertainties were within ± 0.1 s. Upon adjusting the main parameters, such as S_r and F_s, the first phase to move vertically after the low value of air injection was water. When the air velocity increased, the suction force could intrude the coal particles into the suction pipe, but it was still necessary to increase the inlet air velocity to raise them to the level of the separator tank. This further injection could lead to a growth in the buoyancy force, e.g., reduction in the density of the water-coal mixture, and at the same time an upward trend in the shear force between the phases. Therefore, the air velocity for lifting the coal particles was a bit higher than that for pumping water at the same submergence ratio.

The variation in the solid mass flow rate as a function of the superficial air velocity and feeding possibility at the submergence ratio of 0.6 is shown in Fig. 2. These results revealed that, as the air inflow value increased the mass flow rate of the coal particles increases as well. For the three displayed diagrams, the family of curves corresponding to a certain value of F_s is fairly similar to those obtained at other values, but shifted vertically. As illustrated in Fig. 2, considering the increasing rate of the coal transfer, it becomes the compressed air energy is being wasted, so that, for instance, there is still the power to transfer more coal particles at the inlet air velocity equal to 2.4 m/s. This indicates insufficient solids coming rate into the system. Basically, an increase in the value of F_s in the pump can cause the presence of more particles around the entrance of the suction pipe, which consequently raises the possibility of more particles being

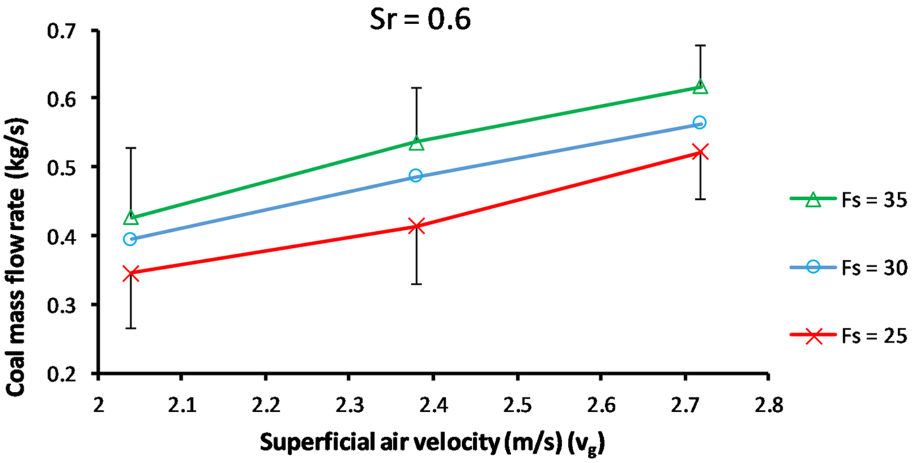

Fig. 2 Particle flow rate in relation to the velocity of inlet gas and feeding solid possibility

sucked into it. This increase in the input can thus lead to an increase in the density of the water–solid mixture, which requires more lifting power to transport them. If the weight force of the water–solid mixture is greater than the sum of the lifting forces, the transmission process will be stopped.

In the previous research by the authors, the minimum injected air velocity to onset the motion and complete the conveying process was considered in detail, and increasing the air injection would only accelerate the transfer of the particles. So, in order to have an optimal performance in solid transfer, much attention must be paid not only to the inflow of compressed air but also to the amount of solid particles intruding. In most of the studies focused on determining the transfer rate of airlift pumps in conveying solid particles, a specific inlet solid rate had been further used to supply solids at the lower pipe section. This can cause the results to be overestimated because it does not correspond to the actual particles coming into the system. It should be emphasized that the increase in the presence of solid particles at the suction pipe inlet is not always beneficial. If the particles accumulate on each other, then more suction force is required to enter them in the transfer process, therefore, the pumping operation will be stopped. Due to the difficult access and the insufficient space around the suction pipe inlet in some projects, such as hydro-borehole mining, the sudden motion of the huge volume of particles towards the entrance of the suction pipe has to be considered in order to keep the transportation continuous and free of errors or clogging, so, the presence of an excessive force is helpful to suspend the particles. For this purpose, some techniques, such as moving impeller (Yoon et al. 2000), high-pressure water injection (Shimizu et al. 1992), and direct impact of compressed air on the particle (Sadatomi et al. 2013) is strongly recommended.

To avoid any mistakes and separate values correctly, only the error bars (2σ) in one direction of the vertical axis are depicted in Fig. 2. It can be inferred from the error bar lines that the fluctuation rate of discharged solid particle at the end of the riser pipe decreases with the increase in the air inflow velocity. Note that the variation in the solid transfer rate does not always depend on the characteristics of the flow regime in the airlift pump, but is also affected by the particle shape. In this context, Enany et al. (2022) found that the more irregular the shape of the particle, the larger the oscillations of the vertical conveying velocity.

Since much research in the field of vertical air–water-solid flow has been conducted in the bubble and slug flow regimes, it has been argued that water is the only phase that carries solids in the three-phase upward flow. However, using experimental tests, Enany et al. (2022) confirmed that air also contributes to the transmission of solids in the churn flow regime because of the higher velocity of the solid phase compared to water. In addition, the fluctuation in water flow has been reported by various researchers under conditions where only water (not solid phase) is being pumped, which is amplified by increasing air velocity. This phenomenon reaches its peak in the churn and annular flow regimes due to the backward motion of the water film (Pagan et al. 2017). In the process of practical tests, the limit of the churn flow regime was not exceeded, and variation in the coal discharge had to be increased by the increase in the inlet air velocity if the particle carrier was the water phase, which is in contradiction with the results presented in Fig. 2. Therefore, in another way, the effectiveness of air in transporting solids and reducing the negative effect of water fluctuation through the greater involvement of continuous air flow is confirmed.

Another significant parameter in the solid particle conveying is the submergence ratio S_r. Two factors should be considered to properly evaluate this parameter. The first one is to avoid reducing the submergence level due to the deduction of the solid weight during sampling, and the second one is the sufficient time for sampling to cover the fluctuations of the water flow. The variation of mass flow of coal particles with superficial air velocity along with submergence ratio is shown in Figs. 3a-b. At a glance, the process of increasing coal transport by increasing the superficial air velocity can be seen for both levels of submergence ratio. The only difference is that at higher submergence ratios, the solids transfer rate is more significant, even with just a lower amount of compressed air. This may be attributed to the longer travel distance for an air bubble to give enough time to transfer its energy to the solid-water mixture. For each submersion ratio, the starting point of vertical particle transfer is different.

As the submergence ratio increases, this point shifts to the left of the horizontal coordinate. This can be explained by the fact that the increased static head at the pump entrance due to the rising water column helping the coal particles to flow earlier. In general, at a constant air flow, reducing the submergence ratio also reduces the amount of water transfer. The reasons for this issue are widely prevalent in the literature. Therefore, for each level of S_r, the lowest amount of injected air was proportional to the time when not only the amount of suction force in the suction pipe was sufficient to start the vertical motion of the coal particles but also the group of coal particles can be transferred to the highest point of the riser pipe. Note that the water velocity at the time of solid transfer initiation is unique and stands in the range of 0.6 to 0.7 m/s for almost all tested submergence levels.

The experimental results presented in Fig. 3a-b also indicate that the start of the vertical coal transfer operation is not affected by the feeding possibility in the pump. The role of this parameter is evaluated more precisely with the aid of one-way valves (backflow prevention), which were installed at the entrance of suction and riser pipes. In general, it was possible to use one valve but to validate the practical results with theoretical equations, it is necessary to know the amount of solid volume fraction (C_V) in each pipe separately. Figure 4a-b is concerned with the present experiments.

Among the three levels of S_r, the water–solid mixture moves upward more regularly (less flow fluctuations) at S_r equal to 0.8, therefore, the data variation also shows a significant reduction. The fluctuation in the upflow has the greatest impact on the suction pipe, so the volumetric coal fraction in it shows more variation compared to the riser pipe. This result also emphasizes that the sampling time must be sufficient so that the results of the solid outflow by the pump are least affected by the moments of max and min transfer. It should be noted that the length of the riser pipe is much longer than the suction pipe, hence, most of the rising particles are located in this area. The growth in the

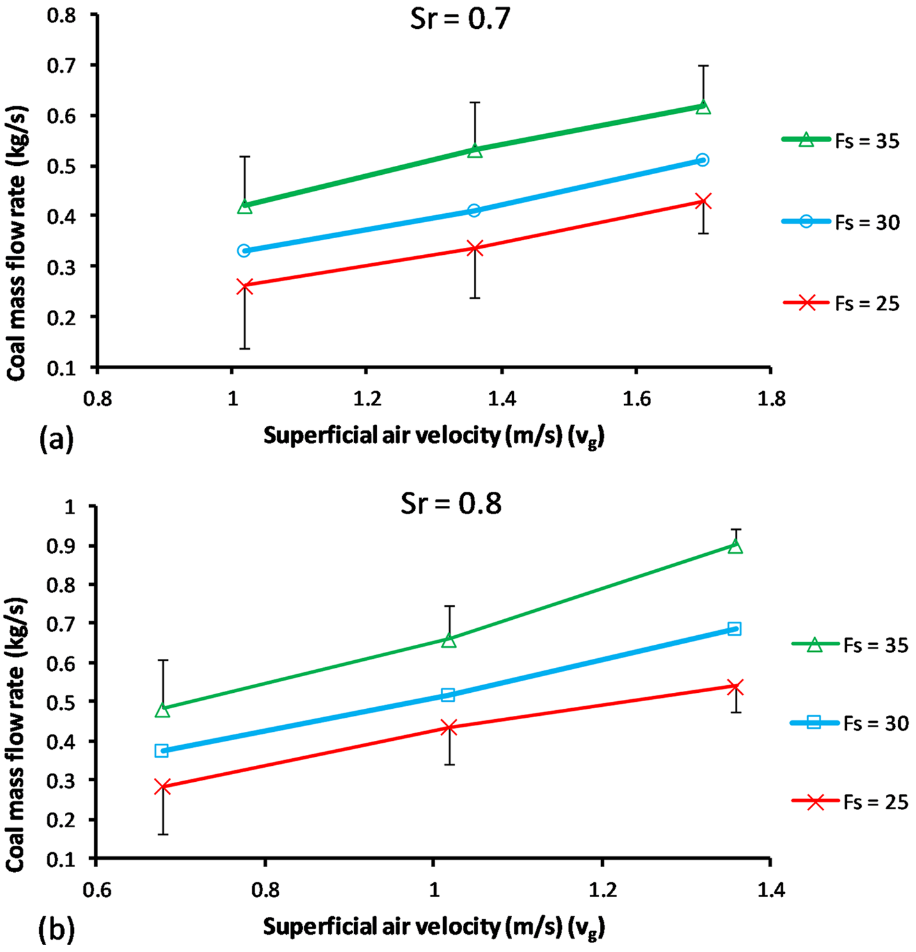

Fig. 3 Effect of the submergence ratio on the solid particle transportation

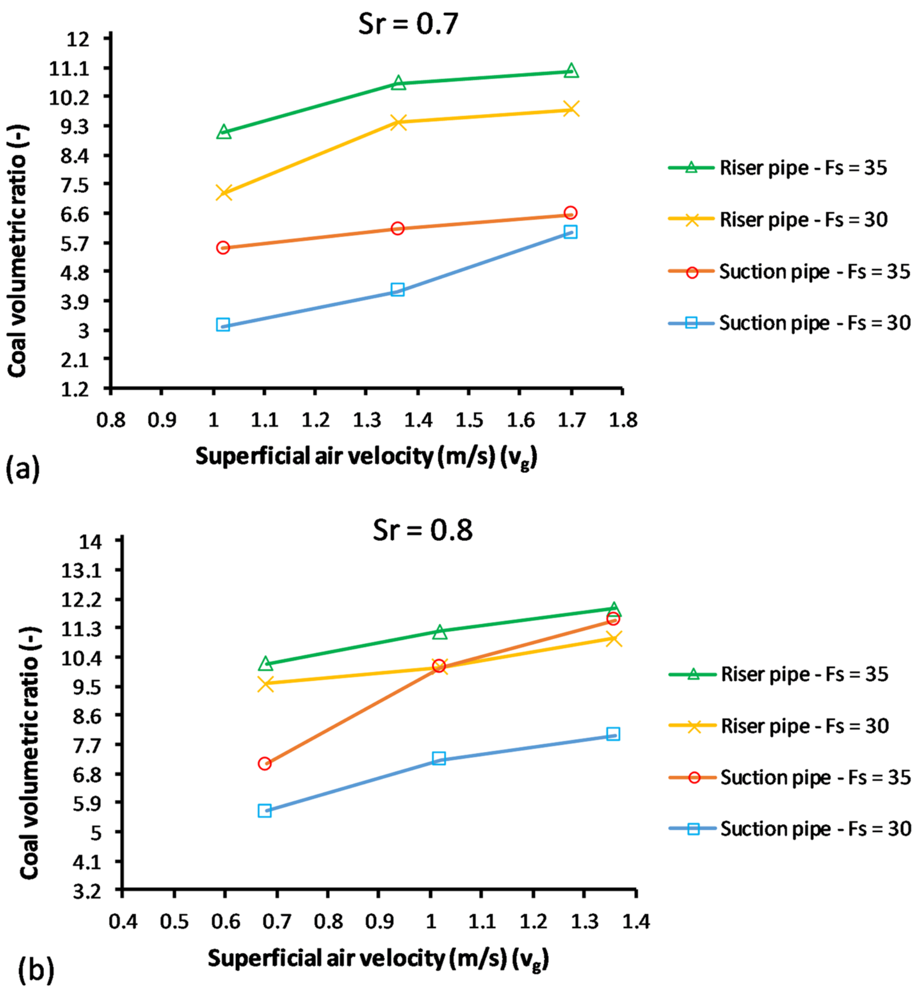

Fig. 4 Solid volume ratio in each part of airlift pump

presence of the particles around the suction pipe inlet due to the placement of more coal in the system clearly shows its positive impact on the increase in the solid volume fraction in both parts of the transportation pipe. In this line, Berg (1992) considered the upper limit of C_V in the airlift pump less than 20%. In the studies reflecting on the efficiency of the airlift pump in carrying solid particles, Mahrous (2012) also evaluated maximum solid volume fraction equal to 20%. To the best of the author's knowledge, the condition higher than 20% has not been yet tested to determine whether the transport process stops or is optimal at all. However, according to the results presented in Fig. 4a-b, the total solid volume fraction is at most 11.7% if the only factor to intrude the particles in the conveying process is the suction force around the suction pipe, and no other external factor helps them.

In conclusion, based on the best results of the present practical experiment and when the other two parameters are constant, increasing the compressed air velocity, submergence ratio, and feeding possibility enhances the displaced coal particles in the range of 15%–30%, 13%–29%, and 19%–25%, respectively. Therefore, the superiority of one independent variable over another cannot be determined with certainty in this experiment. As solid-outflow values subject the normal distribution, the correlation coefficient between the variables can be checked by the Pearson method. Due to the lack of consensus among the researchers in identifying the outliers and the method's sensitivity to this kind of data, Spearman rank method was applied, which the outcomes are presented in Table 1. It should be emphasized that our previously published results were utilized to analysis the correlation between S_r and v_g on the water transfer rate. To ensure that the independent variables do not influence each other, a VIF test was conducted, which the results in Table 1 emphasize non-multicollinearity between them. From Table 1, it is clear that all three independent parameters have a positive impact on the solid transfer rate, i.e., the magnitude of Q_s increases as each independent variable increments. Among them, the level of S_r

Table 1 Spearman correlation factor together with variance inflation factor (VIF) for tested variables

Item	Q_s	Q_w	VIF
v_g	0.202	0.536	3.72
F_s	0.398	–	1.02
S_r	0.752	0.970	3.70

shows the very strongest relationship, whereas the superficial air velocity displays the weakest relationship with the rate at which solids are transferred. Under two-phase flow (water–air) operation condition, the submergence level also shows a very stronger relationship than the injecting air flow. In fact, under three-phase settings, with the addition of a newer parameter, F_s, the degree of correlation for S_r and v_s has been reduced. In total, if there are no restrictions on access to water sources, working at the highest level of S_r will be much less expensive than increasing the injection of compressed air. Moreover, we know that the air velocity and the submergence ratio are controllable, but the particle inflow cannot. In order to achieve a higher mass flow rate of solid, depending on the specific requirement and design of the installation, these magnitudes must be as small as possible. Therefore, airlift pumps should be operated with a large solid particle inflow but without blocking the entrance of the suction pipe and accumulation in the lifting pipe.

3.1 Theoretical background

Over time, much effort has been made to study vertical three-phase flow features for understanding the rheology of solid holdup process. Empirical research has also lead to a wide variety of correlations to explain this process. However, such correlations are valid only under specific flow regimes and justification pump models which provide different predictions once applied to the condition beyond those tested originally. To date, there has been a big challenge to formulate vertical three-phase flows due to their complicated flow behaviors.

In the previous research by the authors (Enany et al. 2022), a new equation was thus offered a new equation to estimate the vertical velocity of solid transportation in an airlift pump. The results on coal particles further confirmed that the effect of friction due to collision with the pipe wall needed to be taken into account to get a more accurate answer for non-spherical particles, especially at high compressed air velocity. Therefore, the previous formula was developed to investigate the transportation of a group of particles. In the mathematical equations, the subscripts s, w, and g are employed for solid, water, and gas, respectively. The superscripts S, R, wg, and swg are also utilized for convenience in distinguishing suction pipe, riser pipe, water–gas flow, and solid–water–gas flow, respectively. The vertical solid transport velocity v_s for the bunch of the particles is thus given by the averaged fluid velocity in the cross-sectional part of the empty pipe v_f corrected for the hindered settling velocity of that fraction v_{Th} (Berg 1992; Wijk 2016), as follows:

$$v_s = v_f - v_{Th} \tag{1}$$

where v_s is the solid-phase velocity (m/s), v_f represents the average velocity of the fluid phase (m/s), and v_{Th} shows the hindered settling velocity of the bunch of particles (m/s). The body of the airlift pump consists of two main parts. One is a suction pipe (with the superscript S in the equations) from the bottom of the vertical pipe to the level of the air jacket, wherein the liquid–solid two-phase mixture flows. The other is the riser pipe (with the superscript R in the equations) from the level of the air jacket to the separator tank, in which the gas–liquid-solid three-phase mixture flows. Therefore, the system of equations should be classified into two parts. Assuming the motion of the particles and the main fluid in the same direction, the vertical solid transport velocity v_s for the bunch of particles for the individual part of the airlift pump is derives from Eq. (1):

$$v_s^S = v_f^S - v_{Th}^S \tag{2}$$

$$v_s^R = v_f^R - v_{Th}^R \tag{3}$$

where v_f^S is equal to water velocity (v_w), and v_f^R is given by:

$$v_f^R = \left(\alpha_w \cdot v_w\right) + \left(\alpha_g \cdot v_g\right) \tag{4}$$

$$\alpha_w = 1 - \alpha_g \tag{5}$$

in which α_w denotes the volumetric fraction of water in the air–water condition (riser pipe). As demonstrated in a previous study (Enany et al. 2022), when the slug flow is maintained in the airlift, the force in the suction pipe is insufficient to start the vertical motion even for one particle in centimeters size, let alone transport it to the end of the riser pipe. Therefore, to estimate the gas void fraction, the equations proposed by Hasan (1988) for Churn flow in the vertical water–gas flow (Eq. (6)) and Giot (1982) for the vertical solid-water–gas flow (Eq. (7)) are considered:

$$\alpha_g^{wg} = \frac{v_g}{1.15\,(v_w + v_g) + 0.345\sqrt{\frac{g \cdot D\left(\rho_w - \rho_g\right)}{\rho_w}}} \tag{6}$$

$$\alpha_g^{swg} = \frac{v_g}{1.2(v_s + v_w + v_g) + v_\infty} \tag{7}$$

where D is the pipe diameter, ρ_g and ρ_w refer to the densities of gas and water, respectively. The density of the gas-phase at the level of the gas injection can be further determined using the following relation as:

$$\rho_g = \frac{P}{\mathrm{R}\,T} \tag{8}$$

here, R stands for the gas constant (287.058 J/kg K) and T is the absolute temperature of the gas phase. In Eq. (7), v_∞ denotes the rising terminal velocity of the churn air bubbles, which can be determined as (Doyle and Halkyard 2007):

$$v_\infty = 1.53\left(\frac{\sigma g^2}{\rho_{\mathrm{sw}}}\right)^{0.25} \tag{9}$$

in which, σ is the surface tension of water against air. Of note, the falling velocity of a group of particles in a fluid is less than the terminal settling velocity of individual particles (Kolev 2005). This effect is called the hindered settling velocity, which is determined by the following equation:

$$v_{\mathrm{Th}}= v_{\mathrm{T}}\,(1 - C_{\mathrm{v}})^{n} \tag{10}$$

where v_{T} is the terminal settling velocity of one solid particle that falls in the center of the pipe with still water (m/s), C_{V} shows the solid volume fraction, and n as given by Richardson and Zaki (1954) reads $n = 2.36$ for $\mathrm{Re}_{\mathrm{p}} > 200$ (Kolev 2005). The particle Reynolds number Re_{p} is thus expressed as:

$$\mathrm{Re}_{\mathrm{p}}=\frac{(v_{\mathrm{T}}\cdot\, \rho_{\mathrm{f}}\cdot\, d_{\mathrm{s}})}{\mu_{\mathrm{f}}} \tag{11}$$

where ρ_{f} is fluid density (kg/m^3), d_{s} is the particle diameter (m), and μ_{f} is dynamic viscosity of the fluid (Pa. sec = kg/m s). The fluid density in the riser pipe is then defined by:

$$\rho_{\mathrm{f}}^{\mathrm{R}}= (\alpha_{\mathrm{w}}\cdot\, \rho_{\mathrm{w}}) + (\alpha_{\mathrm{g}}\cdot\, \rho_{\mathrm{g}}) \tag{12}$$

The solid volumetric fraction in the suction pipe ($C_{\mathrm{V}}{}^{\mathrm{S}}$) and the riser pipe ($C_{\mathrm{V}}{}^{\mathrm{R}}$) is defined as the ratio of the solid phase volume to the total volume of the mixture:

$$C_{\mathrm{V}}^{\mathrm{S}} = \frac{V_{\mathrm{s}}}{V_{\mathrm{s}} + V_{\mathrm{w}}} \tag{13}$$

$$C_{\mathrm{V}}^{\mathrm{R}} = \frac{V_{\mathrm{s}}}{V_{\mathrm{s}} + V_{\mathrm{w}} + V_{\mathrm{g}}} \tag{14}$$

The density of the three-phase flow can now be evaluated from Eqs. (7,8,13, and 14):

$$\rho_{\mathrm{swg}}^{\mathrm{R}}= (\rho_{\mathrm{s}} \cdot C_{\mathrm{V}}^{R})+\left(\rho_{\mathrm{w}} \cdot (1-C_{\mathrm{V}}^{\mathrm{R}}-\alpha_{\mathrm{g}}^{\mathrm{wgs}})\right)+\left(\rho_{\mathrm{g}} \cdot \alpha_{\mathrm{g}}^{\mathrm{wgs}}\right) \tag{15}$$

Due to increased air velocity, the pipe center is occupied by a large gas core as the churn flow continues to develop, and consequently the collision of the particle with the pipe wall is more possible. Considering all the effective and opposing forces during the particle falls in the fluid, the particle terminal settling velocity v_{T} with the influence of the friction between the solid particle and pipe wall is determined by the following equation:

$$v_{\mathrm{T}}=\sqrt{\frac{2V_{\mathrm{p}}\left[4\tau_{\mathrm{s}}-(\mathrm{g}\cdot D\cdot C_{\mathrm{v}}\cdot (\rho_{\mathrm{f}}+\rho_{\mathrm{s}}))\right]}{A_{\mathrm{p}}\cdot C_{\mathrm{D}}\cdot C_{\mathrm{v}}\cdot\rho_{\mathrm{f}}\cdot D}} \tag{16}$$

where V_{p} is the volume of the solid particle (m^3), τ_{s} shows solid shear stress, g is gravity acceleration (m/s^2), D is pipe diameter (m), C_{D} denotes the drag coefficient of the solid particle (-), and A_{p} refers to the cross-section area of the particle in perpendicular to the motion direction. In the related literature, there are several methods to estimate the geometric characters of non-spherical particles, such as particle shape factor, equivalent surface diameter, and sphericity approach, as discussed in detail by King (2002). It is often assumed to be an ideal sphere for calculating the volume and area of solid particles. Since there is no wall friction at the zero-volume fraction of the solids, Eq. (16) has a vertical asymptote at $C_{\mathrm{V}} = 0$ which has no physical meaning. The solid shear stress τ_{s} can be further modeled, as explained in Bartosik (2020):

$$\tau_{\mathrm{s}}=\frac{8.3018\times10^{7}}{\mathrm{Re}^{2.317}} \cdot D \cdot \rho_{\mathrm{s}} \cdot d_{\mathrm{s}}^{2} \cdot \lambda^{1.5} \cdot \left(\frac{\tau_{\mathrm{f}}}{\mu_{\mathrm{w}}}\right)^{2} \tag{17}$$

Note that Eq. (17) uses the air–water mixture velocity $v_{\mathrm{f}}{}^{\mathrm{R}}$ in the riser pipe region. The Reynolds number (Re) is then defined like for the carrier flow in each section of the airlift pump, as follows:

$$\mathrm{Re}^{\mathrm{S}}=\frac{\rho_{\mathrm{w}} \cdot v_{\mathrm{w}} \cdot D}{\mu_{\mathrm{w}}} \tag{18}$$

$$\mathrm{Re}^{\mathrm{R}}=\frac{\rho_{\mathrm{f}}^{\mathrm{R}} \cdot v_{\mathrm{f}}^{\mathrm{R}} \cdot D}{\mu_{\mathrm{w}}} \tag{19}$$

where μ_{w} is the dynamic viscosity of water (Pa.sec). In Eq. (17), a linear volume fraction of the solids (λ) is the ratio of the particle diameter to the mean distance between them, which can be expressed in terms of volumetric fraction in the pipe:

$$\lambda=\frac{1}{\left(\frac{c_{\mathrm{V,max}}}{c_{\mathrm{V}}}\right)^{\frac{1}{3}}-1} \tag{20}$$

Of note, the maximum possible solid fraction ($\mathrm{C}_{\mathrm{V,\,max}}$) occurs when the distance between the particles is zero. The fluid wall shear stress in each part of the airlift pump is also given by:

$$\tau_{\mathrm{f}}^{\mathrm{S}}= f_{\mathrm{w}} \cdot \rho_{\mathrm{w}} \cdot \mathrm{g} \cdot \frac{D}{4} \tag{21}$$

$$\tau_{\mathrm{f}}^{\mathrm{R}}= f_{\mathrm{w}} \cdot \rho_{\mathrm{f}}^{\mathrm{R}} \cdot \mathrm{g} \cdot \frac{D}{4} \tag{22}$$

Here, f_{w} is the Darcy–Weisbach friction factor, which can be found, for instance, with the Colebrook equation or the Moody diagram. Enany et al. (2022) accordingly reported that the average solid transport velocity (v_{sA}) in the airlift pump using the radial air injection method could be defined as:

$$v_{\mathrm{sA}}=\frac{v_{\mathrm{s}}^{\mathrm{S}}\times v_{\mathrm{s}}^{\mathrm{R}}\left(h_{\mathrm{S}}+h_{\mathrm{R}}\right)}{(h_{\mathrm{S}}\times v_{\mathrm{s}}^{\mathrm{S}})+(h_{\mathrm{R}}\times v_{\mathrm{s}}^{\mathrm{R}})} \tag{23}$$

where h_{S} and h_{R} are the length of suction and the riser pipe, respectively. Finally, the solid flow rate (m^3/s) is determined by the following equation:

$$Q_{\mathrm{s}}=A\left(C_{\mathrm{V}}^{\mathrm{S}}+C_{\mathrm{V}}^{\mathrm{R}}\right)v_{\mathrm{sA}} \tag{24}$$

A calculation procedure to obtain the results using the proposed model as follows:

(1) As a first step, based on the known parameters R, P, and T, calculate the ρ_{g} from Eq. (8).
(2) The ρ_{w} and ρ_{s} are known. Calculating the v_{∞} from Eq. (9).
(3) The $\alpha_{\mathrm{g}}^{\mathrm{wg}}$, $\alpha_{\mathrm{g}}^{\mathrm{swg}}$, $v_{\mathrm{f}}^{\mathrm{R}}$, $\rho_{\mathrm{swg}}^{\mathrm{R}}$, and $\rho_{\mathrm{f}}^{\mathrm{R}}$ can be calculated numerically from Eqs. (4), (6), (7), (15), and (12), respectively.
(4) Using Eqs. (21), (22), (20), (18), (19), and (17) in order, for computing solid shear stress τ_{s}.
(5) Before obtaining the value of $v_{\mathrm{Th}}^{\mathrm{S}}$ and $v_{\mathrm{Th}}^{\mathrm{R}}$ from Eq. (10), calculating the values of $v_{\mathrm{T}}^{\mathrm{S}}$, $v_{\mathrm{T}}^{\mathrm{R}}$, and Re_{p} from equations (16) and (11), respectively.
(6) The $v_{\mathrm{s}}^{\mathrm{S}}$ and $v_{\mathrm{s}}^{\mathrm{R}}$ can be calculated numerically from Eqs. (2) and (3), respectively.
(7) Finally, based on the known parameters h_{S}, h_{R}, and pipe cross-section area, compute the value of v_{sA} and Q_{s} from Eqs. (23) and (24), respectively.

3.2 Validity of measured data

In this part, we intend to evaluate the results of this applied research for the coal outflow rate (m^3/s) with Eq. (24). The lack of a unique criterion for calculating the drag coefficient for the irregular-shaped particles, and the diversity of empirical results, have accordingly led to inconsistencies among the researchers. Therefore, this coefficient was determined experimentally under still water conditions with 50 test times, and the average value equal to 0.44 was obtained. In a vertical liquid–gas mixture, it is almost impossible to establish a still fluid condition. As well, using insignificant air injection in a tube with a diameter of 40 cm does not cause the vertical movement of water, which gives the possibilities to test the free falling velocity of some particles. According to the observations here, the coal particle stands for a short distance in the center, and gradually deviates toward the tube wall due to its impact with small air bubbles, therefore, it contacts the tube wall as moving down the standpipe. It means that the results of this test were not acceptable. It should be noted that the measurement method has good accuracy for high-density spherical particles. Overall, the settling velocity of the particle in the water–air mixture is higher than that in water, so the drag coefficient for the calculations was considered lower than that in water. To determine a linear volume fraction of solids (λ), 20 measurements in $D=102$ mm pipe sections with a narrow coal particle size distribution ($d_{\mathrm{s}}=25$–44.5 mm) showed that the maximum volume fraction of the coals closer to $C_{\mathrm{V,max}}\approx 0.6$.

The validation of this experimental results for $\mathrm{S_r}$ equal to 0.8 and 0.7 is presented in Figs. 5a-b through the comparison of the computed outcomes. As seen from this Figure, the curve of the model prediction is parallel or nearly parallel to the observed coal delivery rate values. The most notable difference in both conditions, $\mathrm{F_s}=30$, 35 kg, belongs to the initiation of the coal conveying process, which is related to the low range of v_{g}. In spite of these results at the early stage of transportation, the difference between the calculation on the basis of the fundamental equations of the fluid mechanics and the practical test stands in the range of 5% to 11%, which is considered acceptable in such practical applications.

So far, few studies have been conducted on the effects of solid particles on vertical flow regimes in three-phase flow, especially since the role of non-spherical particles is not well known. Therefore, the type of flow regime at the beginning of coal transportation cannot be determined with certainty. Among the different parameters, the most significant impact on the calculation results was due to the inclusion of shear stress and friction in the coal delivery computation. Figures 6a-b compares the experimental and theoretical values when friction and shear stress do not apply to the calculation process. The computation results under the new conditions, oval marked in Figs. 6a-b, give the best fit to the experimental data.

Regardless of the submergence level, water velocity in the suction pipe at the onset of coal transportation is not so high that the particles driving upward in the center of the pipe, and they are more dispersed over the cross-section. When the velocity of the carrier phase increases, the particles tend to concentrate in the center of the pipe with a vigorous axial velocity, which decreases the particle–wall contact. In the riser tube, the rheology of the solid phase movement also does not always follow a same pattern, because it is highly dependent on the type of the vertical flow regime. In general, as the velocity of the air phase increases, the water and solid phases are driven toward the pipe wall, which augments the collision rate and provides more contact for the solid-water mixture with the pipe wall. The peak of this event can be seen in the annular flow regime, where the large gas core is positioned in the pipe center during the upward motion.

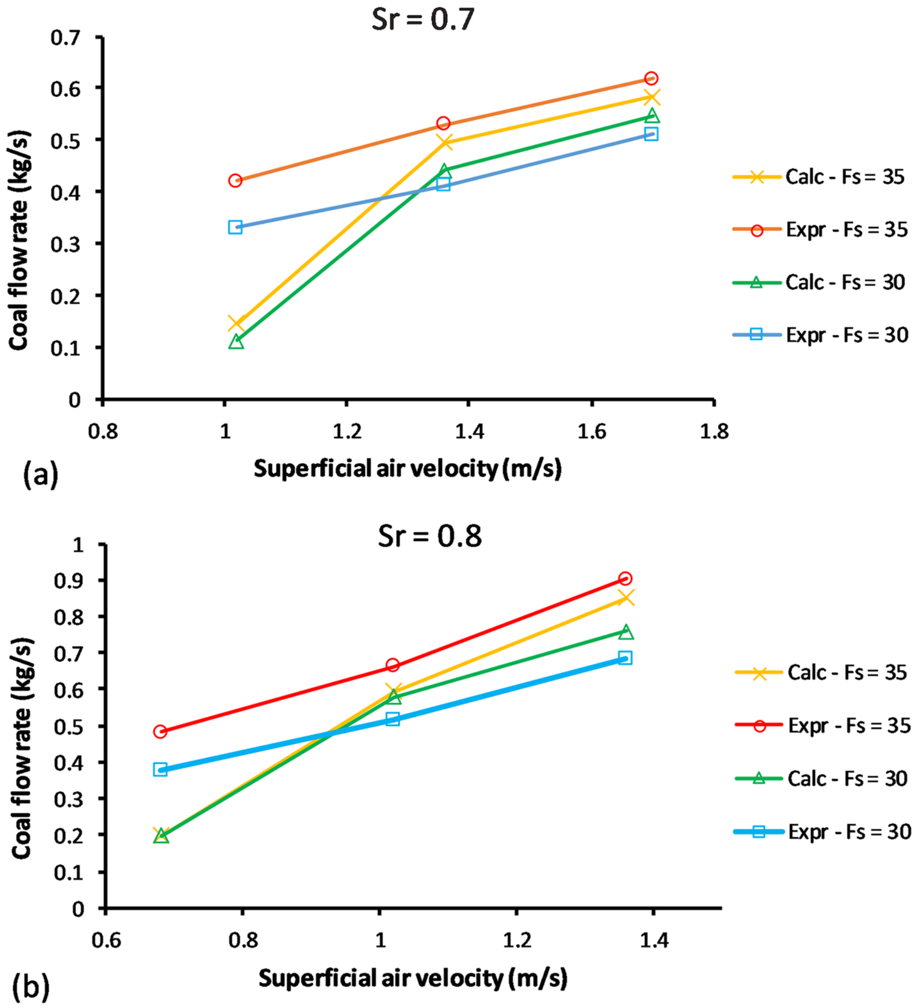

Fig. 5 Comparisons of the particle flow rate calculated by the present method with experimental data

According to above, at the beginning of the solid particle holdup, the role of friction and shear stress in the suction tube is more dominant than that in the riser tube, and this role becomes more effective in the riser tube as the velocity of solid transfer increases because of the growth in the air inflow. Therefore, due to the short length of the suction pipe, it is not recommended to consider the loss related to the friction and the shear stress in the calculations for the initial stages of the solid transfer by an airlift pump with a radial air injection system.

Since the amount of solid volume fraction based on any change in the vertical transfer process has not been provided by other researchers, it was not possible to evaluate our calculation process with the other practical results. The literature review shows that the latest correlation for estimating the performance of airlift pumps in three-phase flow is presented by Kalenik and Chalecki (2018). They determined numerical coefficients for their empirical formulas based on experimental examination of an airlift pump with a 3 cm diameter and 2 m length. The test particle was sand with a graining diameter of 0.8–2.0 mm. Detailed information about the governing equations and model assumptions is beyond the scope of this research. Therefore, only the key equation is presented here (see Eq. (25)).

$$
\begin{aligned}
Q_{\mathrm{s}} = & \frac{H.Q_{\mathrm{g}}}{D^2}[-0.123 + 0.836\frac{Q_{\mathrm{w}}.D^2}{H.K.Q_{\mathrm{g}}} + 5.39 \times 10^{-9}\frac{P_{\mathrm{a}}tm.D^3}{\mu_{\mathrm{g}}Q - w} - 0.034\frac{p_{\mathrm{g}}.D^4}{\rho_{\mathrm{w}}a.Q_{\mathrm{g}}^2} \\
& - 1.236 \times 10^{-5}\frac{P_{\mathrm{g}}.D^4}{\rho_{\mathrm{g}}.q_{\mathrm{g}}^2} - 0.027\frac{P_{\mathrm{g}}.D^4}{\rho_{\mathrm{g}}.q_{\mathrm{g}}^2} + 0.00117\frac{\mu_{\mathrm{w}}}{\mu_{\mathrm{g}}} + 0.29\frac{gD^5}{Q - \mathrm{g}^2}]
\end{aligned}
\tag{25}
$$

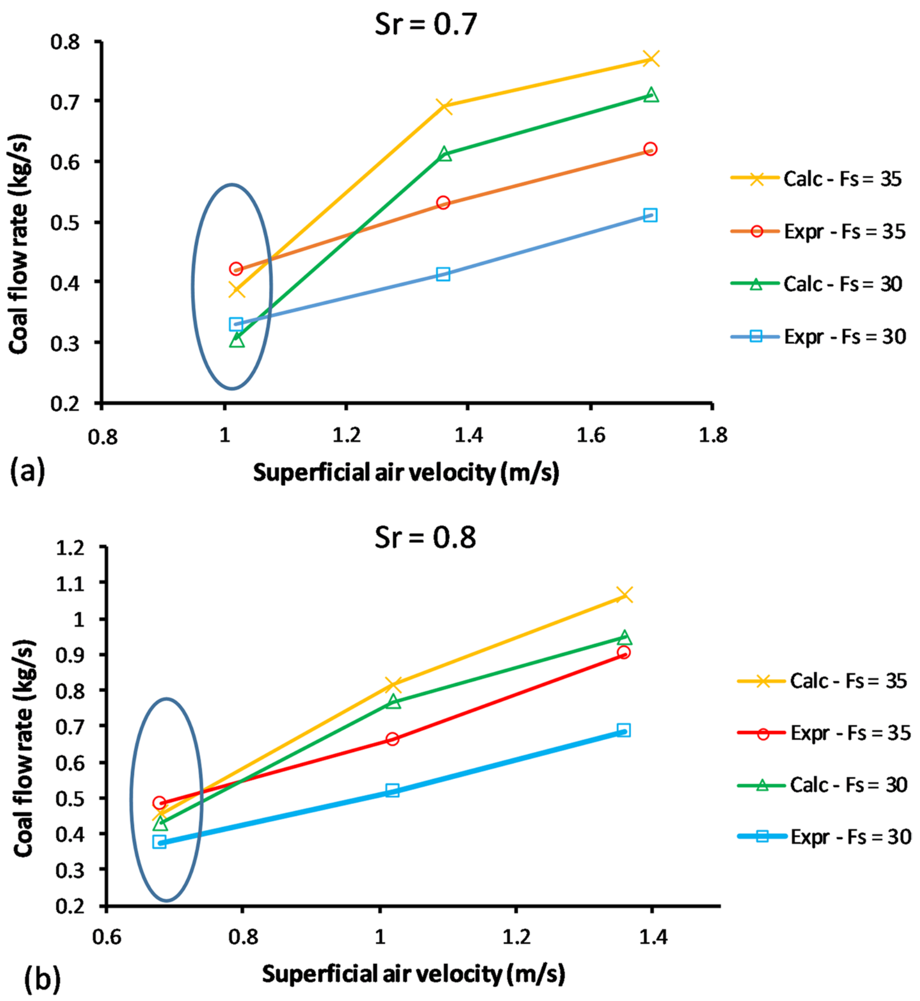

Fig. 6 Comparisons of the particle flow rate calculated without friction by the present method with experimental data

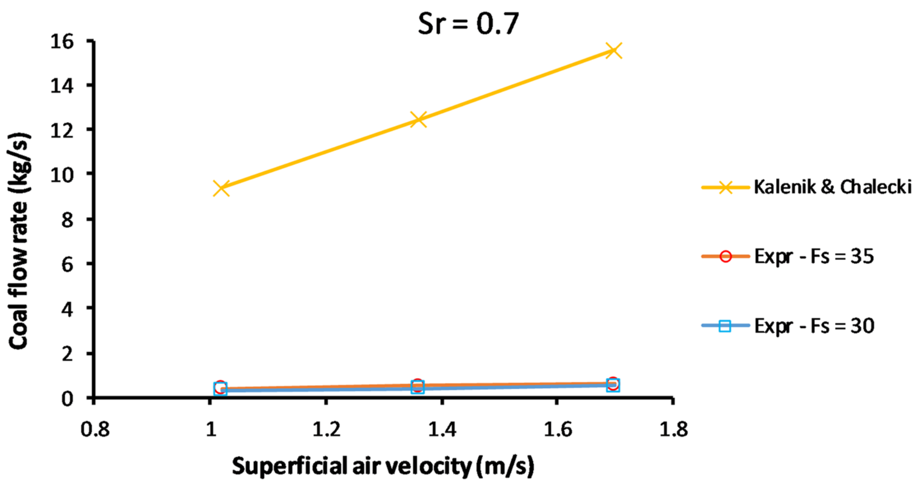

Fig. 7 Comparisons of solid discharged calculated by the Kalenik method with experimental data

At a glance, this model has some shortcomings, such as the lack of any parameters to express the particle dimension and drag coefficient. The delivery head (H) is also given as the distance from the water level to the highest point of the riser pipe. If the submergence ratio is equal to one, then H is equal to zero, and the formula will not receive conclusion.

The results of solid outflow estimation by Kalenik & Chalecki's formula are plotted against our experimental data for a submergence ratio of 0.7 in Fig. 7. It is quite clear that their model overestimates the amount of coal discharges up to 20-fold. This difference is greater than the mean deviation of Q_s, 10%, determined by them when the delivery head is equal to 1.2 m.

4 Conclusions

The present work aims to investigate theoretically and experimentally the conveying centimetric-sized coal particles with an airlift pump. Three types of critical parameters between submergence ratio, air velocity, and feeding coal possibility were systematically examined, and it was found that submergence ratio has strong positive impact on the transport of the tested coal particles. Increasing the level of submergence ratio increases not only the transfer rate of coal particles with less consumption of compressed air, but also causes a continuous delivery rate with fewer fluctuations. Therefore, the optimal submergence ratio for useful particle holdup is more than 0.7, and by raising air inflow, only a faster pumping rate can be achieved. It should be noted that increasing the feeding possibility prevents the loss of compressed air energy, but at the same time increases the possibility of clogging and error in the transfer process. The successful use of one-way valves (backflow prevention) to measure the solid volume fraction in suction and riser pipe showed that in the best case ($S_r = 0.8$, $v_g = 1.36$ m/s, and 35 kg coal) maximum solid fraction during the transportation is about 11.7%. In this study, we also proposed a computation process based on vertical three-phase flow rules to predict solid delivery rate with an airlift pump. The results clearly show that the theoretical model can provide a sufficiently accurate estimation of solid outflow except for the low range of v_g, which refers to the onset of solid transportation. To achieve acceptable calculation accuracy, it is recommended that friction and shear stress are not considered under these conditions. Finally, we found that the correlation proposed by Kalenik and Chaleski is not able to predict the performance of our airlift operation in terms of the solid holdup process.

Supplementary Information The online version contains supplementary material available at https://doi.org/10.1007/s40789-024-00668-y.

Acknowledgements We would like to express our gratitude to the anonymous reviewers of this present manuscript for enhancing the quality of the manuscript.

Author contributions Enany has made contributions to the data curation, formal analysis, investigation, methodology, writing of the work. Drebenstedt has made contributions to the funding acquisition, review and commentary.

Funding This work was supported by the European Research Council (Research Fund for Coal and Steel) under Grant Agreement number 800757.

Data availability The data presented in this study are available on request from the corresponding author.

Declarations

Competing Interests The authors declare that they have no competing of interest. We also emphasize that none of the authors of this paper has a financial or personal relationship with other people or organizations that could adversely influence the content of this work.

References

Abed R, Chadwick E, Ahmed WH (2018) Two-phase flow behaviour in airlift pumps. In: International conference of fluid flow, heat and mass transfer. https://doi.org/10.11159/ffhmt18.168

Al-Maliky SJB (2014) Effect of suction pipe diameter and submergence ratio on air lift pumping rate. AMR 1036:703–707. https://doi.org/10.4028/www.scientific.net/AMR.1036.703

Bartosik A (2020) Validation of friction factor predictions in vertical slurry flows with coarse particles. J Hydrol Hydromech 68:119–127. https://doi.org/10.2478/johh-2020-0005

Berg RR (1992) An analytical and experimental investigation of three-phase flow in airlift pumps used for diamondiferous marine gravel reclamation. Ph.D. Thesis, Cape Town

Doyle RL, Halkyard JE (2007) Large scale airlift experiments for application to deep ocean mining. In: Volume 5: ocean space utilization; polar and arctic sciences and technology; the Robert dean symposium on coastal and ocean engineering; special symposium on offshore renewable energy. ASMEDC, San Diego, California, USA, pp 27–36

Enany P, Shevchenko O, Drebenstedt C (2021) Experimental evaluation of airlift performance for vertical pumping of water in underground mines. Mine Water Environ 40:970–979. https://doi.org/10.1007/s10230-021-00807-w

Enany P, Shevchenko O, Drebenstedt C (2022) Particle transport velocity in vertical transmission with an airlift pump. Fluids 7:95. https://doi.org/10.3390/fluids7030095

Enany P, Shevchenko O, Drebenshtedt C (2023) Evaluation of airlift pump performance for vertical conveying of coal particles. Int J Coal Sci Technol 10:42. https://doi.org/10.1007/s40789-023-00598-1

Fujimoto H, Ogawa S, Takuda H, Hatta N (2003) Operation performance of a small air-lift pump for conveying solid particles. J Energy Res Technol 125:17–25. https://doi.org/10.1115/1.1514498

Fujimoto H, Kubo M, Hama T, Takuda H (2010) Transport phenomena of solid particles in pulsatile pipe flow. Adv Mech Eng 2:121326. https://doi.org/10.1155/2010/121326

Giot M (1982) Three phase flow. In: Hetsroni G (ed) Handbook of multiphase systems. Hemisphere Publishing, Washington, DC

Hasan AR (1988) Void fraction in bubbly, slug and churn flow in vertical two-phase up-flow. Chem Eng Commun 66:101–111. https://doi.org/10.1080/00986448808940263

Hu D, Tang CL, Zhang FH (2012) The effect of air injector on the performance of airlift. Adv Mat Res 516–517:1022–1027. https://doi.org/10.4028/www.scientific.net/AMR.516-517.1022

Kalenik M, Chalecki M (2018) Experimental study of air lift pump delivery rate. Aser 20:221–240

Kassab SZ, Kandil HA, Warda HA, Ahmed WH (2007) Experimental and analytical investigations of airlift pumps operating in three-phase flow. Chem Eng J 131:273–281. https://doi.org/10.1016/j.cej.2006.12.009

Kassab SZ, Abdelrazek AA, Lotfy ER (2022) Effects of injection mechanism on air-water air lift pump performance. Alex Eng J 61:7541–7553. https://doi.org/10.1016/j.aej.2022.01.002

Kato H, Miyazawa T, Timaya S, Iwasaki T (1975) A study of an air-lift pump for solid particles. Bull JSME 18:286–294

King PR (2002) Introduction to practical fluid flow. Elsevier, Amsterdam

Kolev NI (2005) Multiphase flow dynamics 2: thermal and mechanical interactions, 2nd edn. Springer, Berlin

Kumar EA, Kumar KRV, Ramayya AV (2003) Augmentation of airlift pump performance with tapered upriser pipe: an experimental study. J Inst Eng 84:114–119

Mahrous AF (2012) Numerical study of solid particles-based airlift pump performance. WSEAS Trans Appl Theor 7:221–230

Margaris DP, Papanikas DG (1997) A generalized gas-liquid-solid three-phase flow analysis for airlift pump design. J Fluids Eng 119:995–1002. https://doi.org/10.1115/1.2819528

Minagawa H, Shakutsui H, Tomiyama A (2007) Application of a two-phase flow model based on local relative velocity to solid-liquid two-phase flows with coarse particles. J Fluid Sci Technol 2:205–214. https://doi.org/10.1299/jfst.2.205

Pagan E, Williams WC, Kam S, Waltrich PJ (2017) A simplified model for churn and annular flow regimes in small- and large-diameter pipes. Chem Eng Sci 162:309–321. https://doi.org/10.1016/j.ces.2016.12.059

Ramdhani R, Indarto I, Deendarlianto D, Catrawedarma I (2020) Experimental study on the effect of submergence ratio and air flow rate on the characteristics of liquid-gas-solid three-phase airlift pump. In: AIP Publishing. Yogyakarta, pp 040003-1–040003-10

Sadatomi M, Kawahara A, Nishiyama T (2013) Bubble-jet-type air-lift pump for pumping water and sediments deposited on lake and sea beads. Jpn J Multiph Flow 27:141–151. https://doi.org/10.3811/jjmf.27.141

Shimizu YW, Tojo CM, Suzuki M, Takagaki Y (1992) A study on the airlift pumping system for manganese nodule mining. ICOPE, San Francisco, p 490

Wang Z, Deng Y, Pan Y et al (2020) Experimentally investigating the flow characteristics of airlift pumps operating in gas-liquid-solid flow. Exp Therm Fluid Sci 112:109988. https://doi.org/10.1016/j.expthermflusci.2019.109988

Weber M (1974) Fluid conveying technology. Krausskopf-Verlag, Berlin

Wijk JM (2016) Vertical hydraulic transport for deep sea mining. Ph.D. Thesis, University of Delft

Yoon CH, Kwon KS, Kwon OK et al (2000) An experimental study on lab scale air-lift pump flowing solid-liquid-air three-phase mixture. OnePetro, Seattle

Yoshinaga T, Sato Y (1996) Performance of an air-lift pump for conveying coarse particles. Int J Multiph Flow 22:223–238. https://doi.org/10.1016/0301-9322(95)00067-4

Yulistiansah I, Deendarlianto CI (2020) The characteristics of liquid-gas-solid three phase airlift pump for particle diameter mesh 24–20 and 16–12. AIP Publishing, Yogyakarta, p 040005

Zaraki HE, Majidniya M, Abadshapoori MH, Saidi MH (2016) Experimental investigation of flow regime and efficiency of airlift pumps with tapered upriser pipe. Multiph Sci Technol 28:135–152. https://doi.org/10.1615/MultScienTechn.2017018723